The above results show that isothermal polypeptide conformational transitions in the presence of two interacting solvents and an inert solvent can be satisfactorily accounted for with effectively a single parameter model at least in situations where the solvent–solvent interaction is not overwhelming in comparison with the solvent–solute interaction. In certain cases it may also be feasible to determine the respective solvent activities in ternary systems experimentally. This would yield a zero-parameter prediction of polypeptide stabilities in such a system, provided that other factors entering into K_3 (e.g., adsorbate–adsorbate interaction) were unimportant. Additional information concerning, for example, transition enthalpies and fractions of bonded sites at equilibrium require the extension of the above treatment to include the effect of temperature on the phase boundaries. This will be done in a future report.

Acknowledgment. This work was supported by NSF Grant GB 33484.

References and Notes

(1) E.g., G. Perlmann and E. Katchalski, *J. Am. Chem. Soc.*, **84**, 452 (1962); S. M. Bloom, G. D. Fasman, C. deLozé, and E. R. Blout, *ibid.*, **84**, 458 (1962); E. M. Bradbury, A. R. Downie, A. Elliot, and W. Hanby, *Proc. R. Soc. London, Ser. A*, **269**, 110 (1960); N. Lotan, M. Bixon, and A. Berger, *Biopolymers*, **5**, 69 (1967).
(2) F. E. Karasz and G. E. Gajnos, *J. Phys. Chem.*, **77**, 1139 (1973).
(3) R. P. McKnight and F. E. Karasz, *Macromolecules*, **7**, 143 (1974).
(4) P. Dubin and F. E. Karasz, *Biopolymers*, **11**, 1745 (1972).
(5) S. Oae, M. Yokoyama, and M. Kise, *Bull. Chem. Soc. Jpn.* **41**, 1221 (1968); M. Obradovic, T. Solmajer, and D. Hadzi, *J. Mol. Struct.*, **21**, 397 (1974); D. Hadzi and J. Rajvajn, *J. Chem. Soc., Faraday Trans. 1*, **69**, 151 (1973).

Monte Carlo Calculations on Polypeptide Chains. IX. A Study of the Effect of Long-Range Interactions on the Helix–Coil Transition

Darrow E. Neves and Roy A. Scott III*

Department of Biochemistry, The Ohio State University, Columbus, Ohio 43210.
Received November 17, 1975

ABSTRACT: A Monte Carlo statistical mechanical study of the helix–coil transition for a hard-sphere model of poly(L-alanine) has been conducted based on the theory of Lifson and Roig but including the effects of long-range interactions. A stochastic model of the kinetics of the helix–coil transition is presented, and a Monte Carlo simulation of the kinetics based on this model was used to generate equilibrium chain samples, each chain of which consisted of Lifson–Roig weighted sequences of helix and coil residues. Each of the chains in this sample was then used many times by assigning at random specific sterically allowed coil states from a hard-sphere Ramachandran dipeptide map. Unperturbed properties were then calculated using this sample and perturbed properties by using only the non-self-conflicting subset. The properties calculated were the average degree of hydrogen bonding, the average length of a helical sequence, the mean-square end-to-end distance, the mean-square radius of gyration, and the distribution functions for the end-to-end distance and radius of gyration. This study was conducted at chain lengths 10, 34, and 85 residues. Helix–coil transition theory was fit to the perturbed transition curves in an attempt to ascertain if theory could then predict the perturbed values of the dimensions. For the hard-sphere model used in these calculations, it was found that current helix–coil transition theory does not predict the correct perturbed dimensions.

I. Introduction

Since 1951 when Pauling, Corey, and Branson[1] first proposed the α helix as an important conformation for polypeptide chains, there has been a continuing interest in the forces which stabilize this conformation. Schellman[2,3] provided the first theoretical treatments of the helix–coil transition, and his work was followed shortly by various statistical mechanical theories such as those by Gibbs and DiMarzio,[4] Hill,[5] Zimm and Bragg,[6] Peller,[7] and Lifson and Roig.[8] Poland and Scheraga[9,10] and DeVoe[11] have provided recent reviews of this subject. While these theories all differ in their details, they each assign statistical weight parameters to the random coil and helical sequences and then apply standard mathematical techniques to calculate the partition function and the various average properties, such as the fractional hydrogen bonding parameter θ and the average length of helical sequences $\bar{l}$. In their formulation all of these theories take account of the fact that it is more difficult for helical sequences to nucleate than to propagate once they are formed. This causes the helix–coil transition to be highly cooperative and to increase in sharpness with increasing chain length. As a function of chain length, the transition can be divided into three regions. For very short chains the transition is of the all or none type, there being only completely helical and completely random coil molecules present to any appreciable extent at equilibrium. For intermediate chain lengths the transition is of the single helix type, the helix melting from both ends. For long chain lengths the transition proceeds through internal breaks in the helix so that a given molecule has more than one helical sequence.

The general objective of helix–coil transition theory is to explain the dependence of the average properties on chain length, temperature and solvent composition. This is accomplished by treating the various statistical weights as adjustable parameters. Lifson and Roig,[8] for example, introduced the three parameters u, v, and w. u is the statistical weight of a chain unit in the randomly coiled state, i.e., the composite of all configuration space involving internal rotation about a pair of φ and ψ rotational angles for respectively the backbone N–C$^\alpha$ and C$^\alpha$–C′ single bonds, except for a small region designated as the α-helical region. v is the statistical weight of a helical unit which has one or both of its neighboring units in the coil state, and w is that for a helical unit when both of its neighbors are also in the helical state. Since only the

relative values of these statistical weights are of physical significance, the usual procedure is to set $u = 1$ and treat v and w as the adjustable parameters. Then we have[12]

$$v = \exp[-\Delta S_{res}/R] \quad (1)$$

$$w = \exp[\Delta H_{res}/RT - \Delta S_{res}/R] \quad (2)$$

where ΔS_{res} is the entropy gained when a helical unit is converted to a coil unit and ΔH_{res} is the enthalpy change when a helical unit of the w type is converted to a coil unit with the breaking of a hydrogen bond. The enthalpy of conversion of a v type helical unit to a coil unit is usually assumed to be negligible, the predominant contribution to the free energy change being taken to be the increase in conformational entropy ΔS_{res}. Thus v is assumed to be essentially a constant independent of temperature and solvent and dependent only upon the type of amino acid residue. w, of course, is temperature and solvent dependent, the latter being the case since ΔH_{res}, the enthalpy of breaking a hydrogen bond, depends upon the solvent.

Thus we see that this model includes only those kinds of interactions which determine the conformational freedom of a single isolated randomly coiling unit and the near-neighbor interactions between residues which are hydrogen bonded in helical sequences. These are usually referred to in polymer statistics as short-range interactions in distinction from the long-range interactions or excluded-volume effects. In principle these statistical weight parameters can be estimated by the methods of theoretical conformational energy calculations.[13] The statistical mechanical theory of polymer chains including only the effects of short-range interactions has been reviewed by Volkenstein,[14] Birshtein and Ptitsyn,[15] and Flory.[16] The value of such theoretical calculations lies in comparing them to experimental data obtained using ideal or theta-solvent conditions where the effects of long-range interactions or excluded-volume effects are eliminated. This approach is often practical for randomly coiling polymers, and it avoids the theoretical difficulties involved in treating long-range interactions.[17] This approach, however, is not possible for polypeptide chains undergoing a helix–coil transition, because the solvents which induce the transition are usually relatively good solvents for the random coil and are removed from theta conditions, and because inducing the helix–coil transition involves an inherent change in the quality of the solvent. It is reasonable to assume that the resulting random coil would have its average dimensions expanded above those typical of the unperturbed state and would have less conformational entropy per residue than for the unperturbed chain. This should tend to shift the equilibrium more in favor of helical conformations for the perturbed chain relative to that for the unperturbed chain. The effects of long-range interactions on the helix–coil transition have been discussed previously by Ptitsyn[18] and Ptitsyn and Skvortzov.[19]

Because of the importance of including the effects of long-range interactions in the theoretical study of biopolymer conformations and the difficulties involved in doing so, this laboratory has in recent years resorted to the use of Monte Carlo methods.[20-28] To date we have limited these studies to the hard-sphere model of randomly coiling polypeptides and calculated such properties as the mean-square end-to-end distance $\langle r^2 \rangle$, the mean-square radius of gyration $\langle s^2 \rangle$, their higher moments, dipole moments, and the distribution functions for the end-to-end distance and the radius of gyration. The chain length dependencies of these quantities were calculated and compared to their unperturbed counterparts and found to differ considerably, the distribution functions for perturbed chains being of an entirely different nature than those for unperturbed chains.[29] We have also presented evidence that the hard-sphere model does not vastly overemphasize the excluded-volume effect on the dimensions of the random coil.[29] We would expect that long-range interactions would have a considerable effect on the helix–coil transition. This raises the question of whether current theories of the helix–coil transition are valid since they are based only on consideration of short-range interactions.

The primary objective of this paper is to study the effects of long-range interactions on the equilibrium properties of the helix–coil transition, including the calculation of the distribution functions for the chain dimensions for chain lengths 10 and 34. To accomplish this objective we first define a stochastic model theory for the kinetics of the transition, using the Lifson–Roig equilibrium model as a starting point and introducing three parameters to define the residue transition probabilities. We then introduce a Monte Carlo method of simulating the kinetics. The simulation when run out to equilibrium provides a means of generating chain samples with sequences of helix and random coil residues distributed according to the Lifson–Roig weighting scheme. By using the hard-sphere model[22-29] for the polypeptide chain, the coil residues are randomly assigned to specific sterically allowed states. This leads to a large sample of chains which is used to calculate statistical mechanical averages and distribution functions for the chain dimensions both for chains perturbed and unperturbed by long-range interactions. In this study we have investigated chains of length 10, 34, and 85 residues. Chain length 10 is found to be in the all or none region and is short enough so that long-range interactions will be of little significance. Chain length 34 is in the intermediate region in which the transition is of the one-helix type. This chain length is long enough for long-range interactions to be of significance for the hard-sphere model but short enough to avoid internal helical breaks. Chain length 85 is also in the one helix region for small values of v,[30] but the increased chain length will result in an increase in the excluded volume effect. It will be shown in this paper that long-range interactions may have significant effects on the nature of the helix–coil transition which current theory is unable to explain.

II. Models and Methods of Calculation

A. Kinetics Simulation. In their theory of the helix–coil transition, Lifson and Roig[8] defined the statistical weight parameters u, v, and w as configuration intergrals over φ–ψ space, u over the values of φ and ψ in the coil region of a single unit, v over the helical region of such a unit, and w over three consecutive helical units. A polypeptide chain in a given conformation can then be divided into alternating sequences of coil states with statistical weight u^{n_c} and helical states with statistical weights $v^2 w^{n_h-2}$, where n_c and n_h are the number respectively of coil and helical φ–ψ pairs in a sequence. A helical sequence consisting of a single helical φ–ψ pair is assigned a weight v. As mentioned above the usual procedure is to normalize these statistical weights relative to a value of $u = 1$.

To define the stochastic model[31] for the kinetics of the helix–coil transition, we now introduce three transition probability parameters p, q, and α. q is the probability per unit time that a φ–ψ pair of internal rotational angles that are in the coil state will make a transition to those values characteristic of the α-helical state. q is an average probability in that it is not assigned to any particular coil state but to the totality of the coil states. p is the probability per unit time that a unit in a helical state of the v type will make a transition to the coil state. For a sequence of three or more residues in the helical state the probability that they all convert to c states per unit time is $\alpha^{n_h-2} p^{n_h}$ where n_h is the number of φ–ψ pairs in the sequence. Here the parameter α is introduced in recognition of the difficulty of breaking the $n_h - 2$ hydrogen bonds. In this

model it has been assumed that the probability of a c → h transition is q regardless of whether the h is added to an already existing sequence of h states or not. In other words we assume that a residue in a c state must pass across some energy barrier which for a c state is unaffected by the states of the other units in the chain. Of course after passing over this barrier it falls into a deeper well if it is added to an already existing sequence of two or more h states than if it is added to a sequence of only one h state or becomes an isolated h state. For transition from h states to c states the probability p is multiplied by α for those h states involving a hydrogen bond in recognition of the deeper well in which these states lie relative to the top of the energy barrier over which they must pass. By considerations of mass balance we can relate the Lifson–Roig statistical weights u, v, and w to the transition probability parameters p, q, and α. For example, . . . ccc . . . ⇄ . . . chc . . . yields $vu^{-1} = qp^{-1}$ and . . . chhhc . . . ⇄ . . . ccccc . . . yields $v^{-2}w^{-1}u^3 = \alpha p^3 q^{-3}$, which yields with u set to unity

$$q = vp \tag{3}$$

$$\alpha = vw^{-1} \tag{4}$$

Thus, using the Lifson–Roig theory as a basis for the stochastic model requires the introduction of only one additional independent adjustable parameter. For the equilibrium theory by setting $u = 1$, we have the two parameters v and w. For the rate theory we have p, q, and α but with eq 3 and 4 relating them to v and w. Thus if we know v and w, we can calculate α from eq 4 and have a relationship between p and q in eq 3. Just as we could normalize the three parameters u, v, and w by setting $u = 1$, we can normalize p, q, and α by setting $p = 1$. We choose p because it is the largest of the three parameters, i.e., represents the fast h → c process. By choosing $p = 1$ we are introducing a fundamental time unit of duration p^{-1} into the model, namely a time just sufficiently long so that the transition of an isolated h state undergoes a transition to a c state with virtual certainty. In all of the calculations presented in this paper, time will be presented in these units. Other workers[32-34] have formulated kinetics models of the helix–coil transition in terms of rate constants. Our model, which is formulated in terms of transition probabilities, is equivalent to those models.

Since the analytical solution for this model is impractical to use to obtain numerical results except for very short chain lengths,[31] we have adopted a Monte Carlo simulation technique to generate numerical solutions. For chain lengths less than 100, the helix–coil transition for our model is found to be in the one helix region and therefore each molecule will consist of a coil sequence followed by a helical sequence followed by a coil sequence, each sequence being of finite length.[30] In a fundamental time unit, each molecule in the sample may be dealt with as a whole by assigning a probability to each of the new configurations which it may attain; the probability being obtained by use of the weighting scheme discussed above. The selection of the new configuration is made by use of a random number generator. Helical triplets are only allowed to undergo transition to ccc with probability $\alpha p^3 = \alpha$ with $p = 1$. Transitions to such states as hhc, hch, hcc, chh, chc, and cch are not permitted since with $p = 1$ such transitions are impossible. (For example, the probability of hhh → hhc would be equal to $\alpha p(1 - p)^2$.) Sequences of helical states greater than three are handled in a similar manner using this probability scheme and allowing up to as many as two hydrogen bonds per sequence to be broken simultaneously, the probability of three or more breaks being negligibly small. A detailed description of the kinetic simulation will be presented in a future paper.

In addition to generating kinetics data, the Monte Carlo simulation technique can be used to generate various equilibrium samples for use in calculating statistical mechanical averages. In the calculations reported in this paper this was accomplished by starting with a sample of perfectly helical molecules and then running a kinetics simulation to the first equilibrium position of interest. This then served as a starting sample to run a kinetics simulation to the next equilibrium position. This process was repeated progressing from higher average helicity to lower helicity through the entire transition. When each kinetics simulation reached equilibrium, the run was continued for a considerable time at equilibrium. Periodically the sample was saved and added to a growing equilibrium sample until the size of the sample was large enough to use to calculate reasonably accurate average equilibrium properties. In this manner the original kinetic sample is enriched many-fold to produce the equilibrium sample. The random number generator used in this work was the Generalized Feedback Shift Register Pseudorandom Number Algorithim (GFSR).[35] The primitive trinomial $X^{98} + X^{27} + 1$ was used with a 22 bit word size. All calculations presented in this paper were performed on a PDP8-E computer (Digital Equipment Corp.) equipped with 24K of core and a Floating Point Processor.

B. Equilibrium Properties. The equilibrium chain samples generated by the kinetics simulation discussed above serve as the basis for calculating the average properties. First, however, it is necessary to define the equilibrium model. For this purpose we have chosen the hard-sphere model used previously in this laboratory.[22,29] Briefly, in this model the bond lengths and bond angles are held fixed, the peptide bond is fixed in the planar trans configuration, and nonbonded interactions are represented by hard-sphere potential functions. By constructing a Ramachandran dipeptide map of φ vs. ψ, the states of a single chain unit C^α–CO–NH–$C^\alpha H(CH_3)$–CO–NH–C^α are divided into allowed and disallowed states. The allowed states, taken at 10° increments, are then used to represent the totality of coil states for each residue. We have used the dipeptide map for L-alanyl residues used previously[22,29] and thus are treating the case of the hard sphere poly-L-alanine chain. Each of these randomly coiled states is considered to be equally weighted with weight $u/245 = 1/245$ for $u = 1$, there being 245 sterically allowed coil states in the map. Helical states are weighted v or w as in the Lifson–Roig theory. Chains unperturbed by long-range interactions thus have the helical state and the 245 coil states available to each of the n residues. Chains perturbed by long-range interactions can exist only in combinations of helical and coil states for which there are no hard-sphere conflicts in the entire chain.

To include these specific random coil states in the chain sample, we begin with the enriched equilibrium sample discussed above. Each chain in the sample consists of a sequence of n φ–ψ pairs each assigned to either an h or c state. Each member of this sample then has each of its coil φ–ψ pairs assigned by random selection to one of the 245 coil states. Each chain is then classified as self-conflicting or non-self-conflicting. This process is then repeated for each member of the sample numerous times to produce the final sample of chains. Thus each sequence of h and c states produced originally is represented many times in the final sample by chains with the same h and c sequence but with the c states assigned to specific coil states from among the possible 245. Of this final sample of chains, the non-self-conflicting subsample will be used to calculate average properties and distribution functions for chains perturbed by long-range interactions and the entire sample will be used to calculate the corresponding properties for unperturbed chains.

Using this sample the Monte Carlo estimates of the average properties are calculated using the Lifson–Roig weighting scheme but with each specific c state contributing a weight

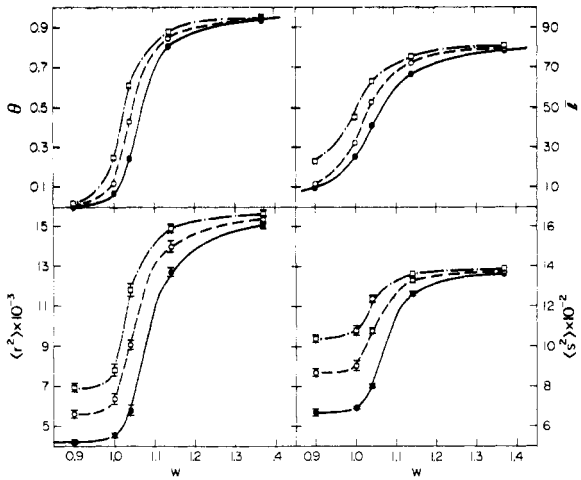

Figure 1. Plots of the fractional hydrogen bonding parameter θ, the average length of a helical sequence $\bar{l}$, the mean-square end-to-end distance $\langle r^2 \rangle$, and the mean-square radius of gyration $\langle s^2 \rangle$, all vs. w at chain length 85, for $v = 0.01$. The closed circles (●) represent the data for unperturbed chains calculated by the Monte Carlo method, the open squares (□) the data for perturbed chains calculated by the Monte Carlo method, and the open circles (○) the data for perturbed chains calculated by the Monte Carlo method but with the radii of all atoms reduced by one-half. The solid lines (—) are the theoretical curves for the four parameters. The dashed dot lines (– · –) and the dashed lines (- - -) are constructed through the experimental points.

$u/245 = 1/245$. The weight for each chain being a product of the factors 1/245, v, and w, one factor for each amino acid residue. The chain is considered to begin at the α-carbon atom of the N-terminal residue and end at the α-carbon atom of the C-terminal residue, the amino group at the N terminus, the carboxyl group at the C terminus, and the H and R group on the first and last residues being neglected. These end effects are negligible except for very short chain lengths. If w_i is the statistical weight for the ith member of the sample, the average property $\langle x \rangle$ is calculated according to eq 5.

$$\langle x \rangle = \sum w_i x_i / \sum w_i \qquad (5)$$

where the summation is over all chains in the sample for unperturbed chains and over the non-self-conflicting subsample for chains perturbed by long-range interactions. The average properties calculated are θ, the fractional hydrogen bonding parameter, $\bar{l}$, the average length of a helical sequence, $\langle r^2 \rangle$, the mean-square end-to-end distance, and $\langle s^2 \rangle$, the mean-square radius of gyration. The distribution functions $W(\rho)$ for the reduced end-to-end distance and $W(\sigma)$ for the reduced radius of gyration were calculated for both perturbed and unperturbed chains by the method described previously by Knaell and Scott.[28] Here $\rho = r/\langle r^2 \rangle^{1/2}$ and $\sigma = s/\langle s^2 \rangle^{1/2}$.

III. Results

In Figure 1 is plotted the four transition curves, θ, $\bar{l}$, $\langle r^2 \rangle$, and $\langle s^2 \rangle$, vs. w for chain length 85 and $v = 0.01$. The Monte Carlo unperturbed points are in excellent agreement with the theoretical calculations for all parameters which assures us that our sample is representative. Similar agreement was also found for the unperturbed properties at chain length 10 and $v = 0.01$ and chain length 34 with $v = 0.01$ and 0.032; however, these results are not shown. As can be seen, the perturbed curves are shifted to the left, i.e., shifted to a higher transition temperature, for all properties. This shift of the perturbed transition curves is due to the effect of long-range interactions. As can be seen, agreement between unperturbed and perturbed properties is found only for large values of w, where the molecules are nearly all perfect helices.

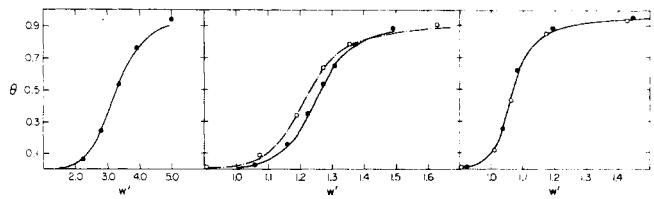

Figure 2. Plots of the best fit of the parameters v' and w' (see text) to the perturbed data for θ. Shown are the plots for chain lengths 10, 34, and 85 in the left, middle, and right boxes, respectively. The solid lines (—) and the dashed dot line (– · –) are the theoretical curves calculated using the best fitting v' and range of w'. The solid circles (●) represent the data for perturbed chains, the open circles (○) in the middle box represent perturbed data generated at $v = 0.032$, and the open circles (○) in the last box represent perturbed data with all radii reduced by one-half.

While interesting, these results do not imply a breakdown of helix–coil transition theory. The transition curve data for θ which an experimentalist measures is for chains which are expanded due to long-range interactions, i.e., the data are perturbed, and the v and w parameters are freely adjusted to obtain a best fit.[36] After one has obtained a best fitting value of v' and range of w' (v' and w' are used to distinguish these quantities from the theoretical v and w discussed above), transition curves can be calculated for $\bar{l}$, $\langle r^2 \rangle$, and $\langle s^2 \rangle$ using methods developed by Flory.[16] The question which will be considered here is will helix–coil transition theory accurately predict perturbed dimensions? In Figure 2 is shown transition curves for chain lengths 10, 34, and 85. The solid circles at all chain lengths represent data generated using $v = 0.01$. The open circles at chain length 34 represent $v = 0.032$ and the open circles at chain length 85 represent $v = 0.01$ but with the radii of all atoms decreased by one-half. We now assume that this perturbed data at all three chain lengths is experimental data and use theory to arrive at a v' and a range of w' which best fits these data. Again referring to Figure 2, at chain length 10 the v' which best fits the data is $v' = 0.007$. At chain length 34, the v' which best fits the solid and open circles are 0.008 and 0.013, respectively. At chain length 85, the v''s for the open and closed circles are respectively 0.013 and 0.0115, the difference between the theoretical curves for these two values of v' being so small that only one theoretical curve is shown. As can be seen in Figure 2, theory fits our perturbed data quite well for all cases investigated although one value of v' will not fit the data at all three chain lengths.

Using the appropriate v' and range of w' for each chain length, the theory was then used to generate transition curves for $\bar{l}$, $\langle r^2 \rangle$, and $\langle s^2 \rangle$. These results are shown in Figures 3, 4, and 5, for chain lengths 10, 34, and 85, respectively, graphed as a function of θ in each case. Figure 3 shows the perturbed data along with the transition curves for $\bar{l}$, $\langle r^2 \rangle$, and $\langle s^2 \rangle$ predicted by theory for chain length 10. The solid lines are the transition curves predicted by theory using the v' and range of w' as described above. As can be seen, theory does a reasonably good job of predicting $\bar{l}$, the error being no more than 5% for any point. The experimental points for $\langle r^2 \rangle$ and $\langle s^2 \rangle$ are shown with 90% confidence limits with the broken line constructed through the experimental points. For both $\langle r^2 \rangle$ and $\langle s^2 \rangle$, agreement between experiment and theory is found only for values of θ close to 1. Disagreement grows as the dimensions expand more rapidly than theory predicts as θ decreases from 1 to 0. Of course for this short chain length, disagreement between experiment and theory is small, less than 14% for $\langle r^2 \rangle$ and less than 10% for $\langle s^2 \rangle$ at θ equal to 0.

In Figure 4 are shown the transition curves for chain length 34 for v' equal to 0.008 and 0.013 indicated by the solid and short dashed lines, respectively. For $\bar{l}$, theory does an excellent job at predicting the transition curve for v' equal to 0.013. For

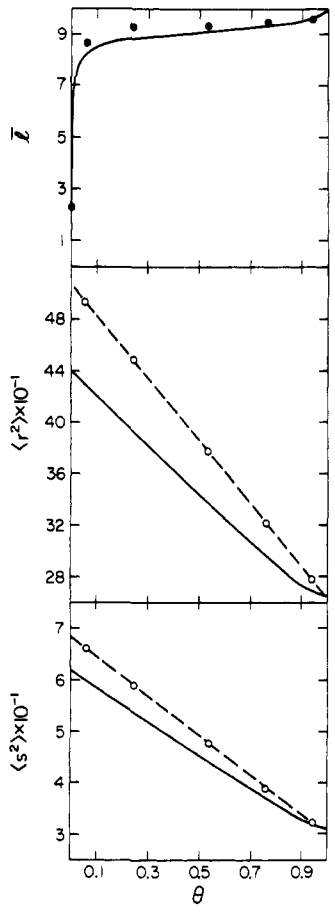

Figure 3. Plots of $\bar{l}$, $\langle r^2\rangle$, and $\langle s^2\rangle$ vs. θ for chain length 10. The open and closed circles are the perturbed data with the dashed line constructed through these points for $\langle r^2\rangle$ and $\langle s^2\rangle$. The 90% confidence limit is smaller than the experimental points shown. The solid lines are the theoretical estimates of these parameters calculated using the best fitting v' and range of w'.

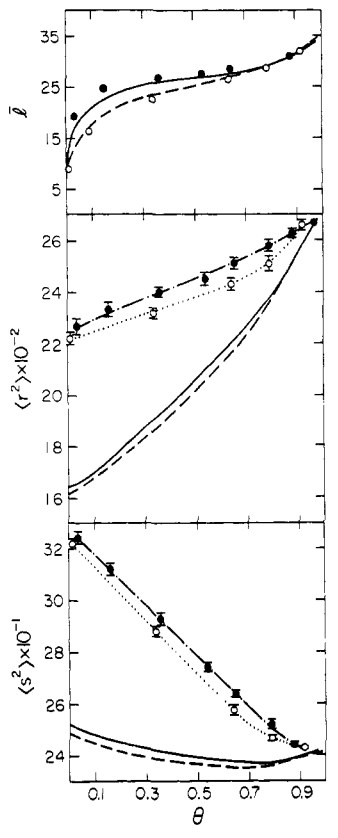

Figure 4. Plots of $\bar{l}$, $\langle r^2\rangle$, and $\langle s^2\rangle$ vs. θ for chain length 34. The solid circles represent perturbed data calculated using a $v = 0.01$. The dashed dot lines are constructed through these points and the solid lines represent the theoretical estimates of the parameters. The open circles represent perturbed data calculated using $v = 0.032$. The dotted lines are constructed through these points and the dashed lines represent the theoretical estimates of the parameters.

$v' = 0.008$, theory also does a reasonably good job, the error being no more than 10% for any point. The experimental points for $\langle r^2\rangle$ and $\langle s^2\rangle$ are shown with 90% confidence limits for $v' = 0.008$ and 0.013. As can be seen, there is little difference in the dimensions predicted by theory between $v' = 0.008$ and 0.013 and also small difference between the curves constructed through the experimental points for $v' = 0.008$ and 0.013. Experimental and theoretical values agree at θ near 1 as expected, but disagreement is apparent even at large values of θ and grows as the helicity approaches 0. The experimental points indicate that $\langle r^2\rangle$ decreases more slowly than predicted by theory, the difference being approximately 26% at $\theta = 0$ for both values of v'. The experimental points indicate that $\langle s^2\rangle$ increases more rapidly than predicted by theory as θ decreases from 1 to 0. In this case the difference between theory and experiment is approximately 23% at $\theta = 0$ for both values of v'.

In Figure 5 is shown the transition curves for chain length 85 with $v' = 0.013$ for the full radii case and $v' = 0.0115$ for the half-radii case. The transition curves predicted by theory for $\bar{l}$, $\langle r^2\rangle$, and $\langle s^2\rangle$ using these two values of v' are essentially the same and are shown as one solid line in Figure 5. Here theory does a less satisfactory job of predicting the transition curve for $\bar{l}$ than at the shorter chain lengths. Good agreement is found only at the extreme ends of the transition while in the middle of the transition, the disagreement is as high as 20%. The experimental points for $\langle r^2\rangle$ and $\langle s^2\rangle$ are shown, with 90% confidence limits for both the full and half-radii cases. For both of these cases for both $\langle r^2\rangle$ and $\langle s^2\rangle$, the experimental points indicate that the dimensions decrease less rapidly than predicted by theory. Good agreement is found between experiment and theory only for values of θ near 1, and significant differences between experiment and theory are apparent for values of θ not far removed from 1. For $\langle r^2\rangle$ the disagreement between theory and experiment is approximately 40% for the full radii case and 27% for the half-radii case at $\theta = 0$. For $\langle s^2\rangle$, the disagreement between theory and experiment is approximately 36% for the full radii case and 25% for the half-radii case at $\theta = 0$.

In Figure 6 are shown the distribution functions $W(\rho)$ vs. ρ and $W(\sigma)$ vs. σ for unperturbed and perturbed chains of length 10. The distribution function for the pure random coil has been investigated elsewhere,[29] and the distribution function for the pure helix would be a δ function located at ρ or σ equal to unity. Referring to columns 1 and 2 in this figure, we see the most striking difference between the unperturbed and perturbed distribution functions at the random coil end of the transition. For this extremely short chain length we do not expect, and indeed do not find, much difference in the value of θ at the same value of w. It is clear however that the unperturbed and perturbed samples are different. For the unperturbed sample at the smallest value of w, the distribution function is approaching the non-Gaussian limiting form discussed in a previous paper;[29] however, here there is a distinct helical peak near ρ equal to 0.8. For the perturbed sample $W(\rho) \rightarrow 0$ as $\rho \rightarrow 0$. As the transition proceeds from coil to helix, the differences between the unperturbed and perturbed samples become less noticeable. In the second row for both unperturbed and perturbed samples, the helix peak has grown larger and has moved toward $\rho = 1$, although the helix peak

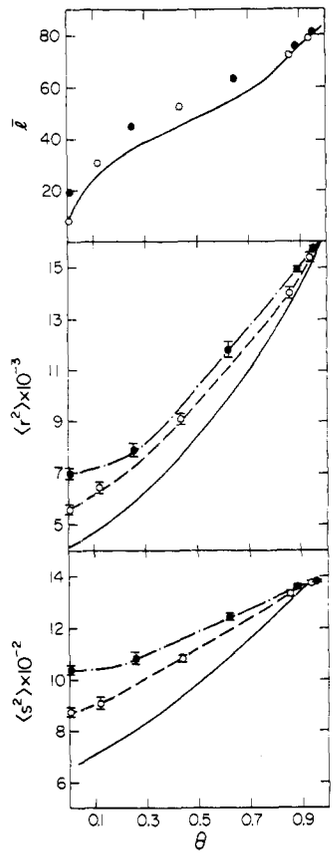

Figure 5. Plots of $\bar{l}$, $\langle r^2 \rangle$, and $\langle s^2 \rangle$ vs. θ for chain length 85. The solid circles represent perturbed data with the dashed dot line constructed through these points. The open circles represent perturbed data with the radii of all atoms reduced by one-half. The dashed lines are constructed through these points. The solid lines are the theoretical estimates of the parameters.

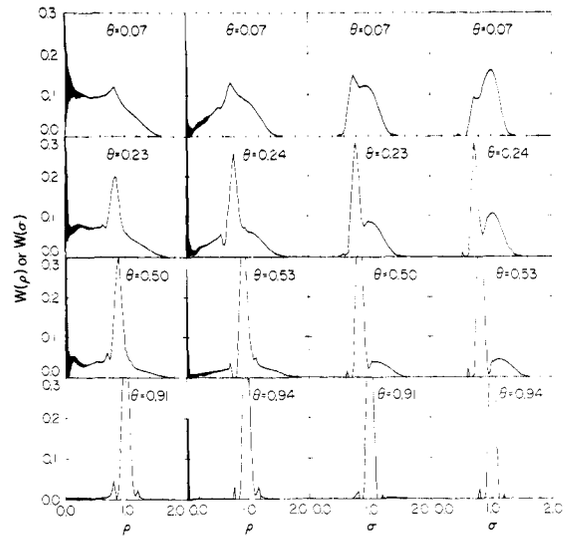

Figure 6. Plots of $W(\rho)$ vs. ρ in columns 1 and 2 and $W(\sigma)$ vs. σ in columns 3 and 4 for chain length 10. Columns 1 and 3 are plots of unperturbed chains and columns 2 and 4 are plots of perturbed chains.

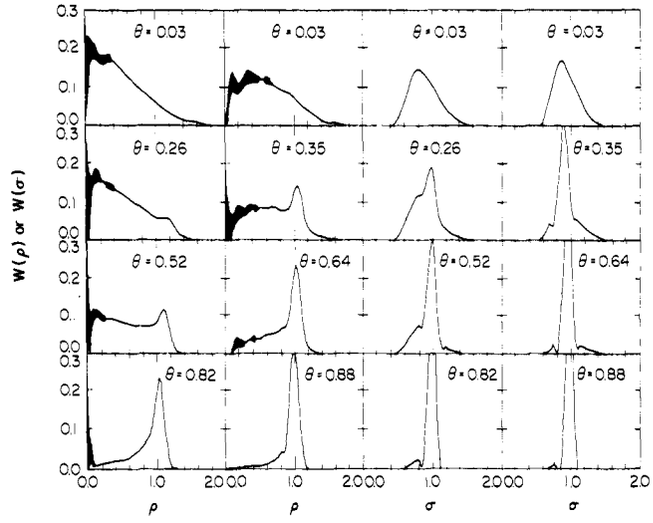

Figure 7. Plots of $W(\rho)$ vs. ρ in columns 1 and 2 and $W(\sigma)$ vs. σ in columns 3 and 4 for chain length 34 and $\upsilon = 0.01$. Columns 1 and 3 are plots of unperturbed chains and columns 2 and 4 are plots of perturbed chains.

is larger and sharper for the perturbed case. Also distinct shoulders are forming on either side of the helix peak. In the third row we see that the helix peak dominates both distribution functions with the shoulders on either side of the peak more distinct and the center of the peak closer to $\rho = 1$. In the bottom row, the unperturbed and perturbed distribution functions are differentiated only by the position of the helix peak which is closer to 1 for the unperturbed case and by the shape of the shoulders around the helix peak. We see a similar phenomenon in columns 3 and 4 for the reduced radius of gyration. The helix peaks are located at approximately 0.8 for both the unperturbed and perturbed case. As the transition proceeds from coil to helix, the helix peak moves to the right toward $\sigma = 1$ and grows at the expense of the coil peak. Concomittantly, distinct shoulders form on either side of the helix peak. In row 4 it can be seen that there is essentially no difference in the distribution functions of the unperturbed and perturbed samples.

In Figure 7 are shown the distribution functions for chain length 34, $\upsilon = 0.01$. Again the distribution function for the pure random coil has been investigated elsewhere[29] and the distribution function for the pure helix would be a δ function located at ρ or σ equal to unity. For this longer chain length, significant differences are found in the unperturbed and perturbed values of θ at identical values of w. This can be seen by observing the values of θ in each row. Also the differences between the unperturbed and perturbed distribution functions for both $W(\rho)$ and $W(\sigma)$ are obvious through the entire region of the transition shown in the figure. For the end-to-end distance, the distribution function for the unperturbed case at small θ is closer to Gaussian behavior than for chain length 10, while the distribution function for the perturbed case is very similar to that found for the pure random coil.[29] In row 2, a helix peak has formed for both the unperturbed and perturbed case. The helix peak in the perturbed distribution function is of course larger and sharper than that for the unperturbed case. In row 4, the helix peak dominates both distribution functions although a vestige of the coil peak remains particularly for the unperturbed case. The helix peak is centered at $\rho = 1$ for both cases but is substantially larger for the perturbed case. In columns 3 and 4 are found the distribution functions for $W(\sigma)$ vs. σ. In row 1 the distribution functions have a well defined coil peak for both cases at $\sigma < 1$. As the transition increases in helicity, a helix peak appears close to $\sigma = 1$. This helix peak is larger and sharper for the perturbed case than for the unperturbed case. In row 3, distinct shoulders have formed around the helix peak for both the unperturbed and the perturbed cases. Finally, in row 4 the distribution functions for the unperturbed and perturbed cases are virtually indistinguishable. As far as the authors are aware, these

are the first reported calculations of distribution functions for any model of the helix–coil transition for either perturbed or unperturbed chains.

IV. Discussion

The results shown indicate that for the model used in this study, helix–coil transition theory is not capable of correctly predicting the dimensions of the polymer undergoing a helix–coil transition. Currently existing theories of the helix–coil transition, such as the Lifson–Roig theory, all neglect the effect of long-range interactions. In the chain length region investigated in this paper, it has been shown that there is a nontrivial, chain length dependent excluded volume effect on the helix–coil transition. In a recent publication,[29] the authors have shown that the hard-sphere model does not vastly over-emphasize the excluded volume effect for the random coil. Nevertheless, an effort was made to determine what effect variations in the hard-sphere potential, i.e., variations in the radii, would have on the above conclusions. It was found, although not shown here, that small variations of the radii in the range 5 to 10% would change the numbers slightly but would not effect the overall conclusions. Accordingly, a drastic reduction in the radii of 50% was made to demonstrate that the excluded volume effect would be reduced by using the smaller radii but that this reduction would not be sufficient to change the conclusions reached using the normal radii. This calculation was conducted at chain length 85 and the results are shown in Figures 1, 2, and 5. As expected, the dimensions for the half-radii case lie between the dimensions for the full radii case and the dimensions predicted by theory. Furthermore, although the radii were reduced by 50%, the reduction in the excluded volume effect was less than 50% for both $\langle r^2 \rangle$ and $\langle s^2 \rangle$.

In conclusion we would like to suggest an experimental approach to evaluating the importance of long-range interactions in the helix–coil transition and to test the validity of current theories. If the theories are correct, it should be possible to fit them to experimental data over a large range of chain lengths. It is essential that very short chain lengths be included where the effects of long-range interactions are negligible as well as intermediate and very long chain lengths where the effect should become more important. It is also important that the theories be fit with a single consistent set of parameters not only to the experimental transition curves but also to the chain dimensions. The inability of the theories to pass such as experimental test would suggest that long-range interactions, as well as other possible effects not taken into account by the theories, are important.

Acknowledgment. This work was supported by a grant (GB-39851) from the National Science Foundation. One of us (R.A.S.) is also a United States Public Health Service Career Development Awardee (GM-38-75/6).

References and Notes

(1) L. Pauling, R. B. Corey, and H. R. Branson, *Proc. Natl. Acad. Sci. U.S.A.*, **37,** 205 (1951).
(2) J. A. Schellman, *C . R. Trav. Lab. Carlsberg, Ser. Chim.*, **29,** 223, 230 (1955).
(3) J. A. Schellman, *J. Phys. Chem.*, **62,** 1485 (1958).
(4) J. H. Gibbs and E. A. DiMarzio, *J. Chem. Phys.*, **30,** 271 (1959).
(5) T. L. Hill, *J. Chem. Phys.*, **30,** 383 (1959).
(6) B. H. Zimm and J. K. Bragg, *J. Chem. Phys.*, **31,** 526 (1959).
(7) L. Peller, *J. Phys. Chem.*, **63,** 1194, 1199 (1959).
(8) S. Lifson and A. Roig, *J. Chem. Phys.*, **34,** 1963 (1961).
(9) D. Poland and H. A. Scheraga, "Theory of Helix–Coil Transitions in Biopolymers", Academic Press, New York, N.Y., 1970.
(10) D. Poland and H. A. Scheraga, "Poly-α-amino Acids", G. D. Fasman, Ed., Marcel Dekker, New York, N.Y., 1967, p 391.
(11) H. DeVoe, "Structure and Stability of Biological Macromolecules", S. N. Timasheff and G. D. Fasman, Ed., Marcel Dekker, New York, N.Y., 1969.
(12) Reference 9, p 19.
(13) A. J. Hopfinger, "Conformational Properties of Macromolecules", Academic Press, New York, N.Y., 1973.
(14) M. V. Volkenstein, "Configurational Statistics of Polymeric Chains", Interscience, New York, N.Y., 1963.
(15) T. M. Birshtein and O. B. Ptitsyn, "Conformations of Macromolecules", Interscience, New York, N.Y., 1966.
(16) P. J. Flory, "Statistical Mechanics of Chain Molecules", Interscience, New York, N.Y., 1969.
(17) H. Yamakawa, "Modern Theory of Polymer Solutions", Harper and Row, New York, N.Y., 1971.
(18) O. B. Ptitsyn, *Biofizika*, **7,** 257 (1962).
(19) O. B. Ptitsyn, and A. M. Skvortzov, *Biofizika*, **10,** 6 (1965).
(20) K. K. Knaell and R. A. Scott III, *J. Chem. Phys.*, **54,** 566 (1971).
(21) K. K. Knaell and R. A. Scott III, *J. Chem. Phys.*, **54,** 3556 (1971).
(22) H. E. Warvari, K. K. Knaell, and R. A. Scott III, *J. Chem. Phys.*, **55,** 2020 (1972).
(23) H. E. Warvari, K. K. Knaell, and R. A. Scott III, *J. Chem. Phys.*, **56,** 2903 (1972).
(24) H. E. Warvari and R. A. Scott III, *J. Chem. Phys.*, **57,** 1146 (1972).
(25) H. E. Warvari and R. A. Scott III, *J. Chem. Phys.*, **57,** 1154 (1972).
(26) H. E. Warvari, K. K. Knaell, and R. A. Scott III, *J. Chem. Phys.*, **57,** 1161 (1972).
(27) K. K. Knaell, H. E. Warvari, and R. A. Scott III, "Conformation of Biological Molecules and Polymers", E. D. Bergmann and B. Pullman, Ed., The Israel Academy of Sciences and Humanities, Jerusalem, 1973, p 777.
(28) K. K. Knaell and R. A. Scott III, *Polym. Prepr., Am. Chem. Soc., Div. Polym. Chem.*, **14,** 157 (1973).
(29) D. E. Neves and R. A. Scott III, *Macromolecules*, **8,** 267 (1975).
(30) R. L. Jernigan and J. A. Ferretti, *J. Chem. Phys.*, **62,** 2519 (1975).
(31) R. A. Scott III, unpublished results.
(32) G. Schwarz, *Biopolymers*, **6,** 873 (1968).
(33) T. R. Chay and C. L. Stevens, *Macromolecules*, **8,** 531 (1975).
(34) J. A. Ferretti, B. W. Ninham, and V. A. Parsegian, *Macromolecules*, **3,** 34 (1970).
(35) T. G. Lewis and W. H. Payne, *J. ACM*, **20,** 3, 456 (1973).
(36) R. T. Ingwall, H. A. Scheraga, N. Lotan, A. Berger, and E. Katchalski, *Biopolymers*, **6,** 331 (1968).